Journal of Materials Chemistry B

Accepted Manuscript

ROYAL SOCIETY OF CHEMISTRY

www.rsc.org/materialsB

Journal of
Materials Chemistry B

Cite this: DOI: 10.1039/c0xx00000x

www.rsc.org/xxxxxx

Full Paper

Novel nanoassembled doxorubicin prodrug with a high drug loading for anticancer drug delivery†

Zhigang Xu[a, b], Kelin Zhang[a], Cuilan Hou [c], Dongdong Wang[a], Xiaoyan Liu[a], Xiujuan Guan[a] Xiaoyu Zhang*[, c] and Haixia Zhang*[, a]

Received (in XXX, XXX) Xth XXXXXXXXX 20XX, Accepted Xth XXXXXXXXX 20XX
DOI: 10.1039/b000000x

We report here a novel doxorubicin (DOX) prodrug that reduces the proportion of inactive materials and minimizing drug leak. In aqueous solutions, the resulting DOX prodrug could spontaneously form stable micelles with diameters of ~ 80 nm with a DOX loading content as high as ~ 40 wt%. The subsequent cytotoxicity and cell internalization behavior indicated that the resulting prodrug could show a high *in vitro* anticancer efficacy. We believe that this strategy could be developed to design prodrugs of various anticancer drugs and thus offer new prodrugs for cancer therapy.

Introduction

In recent years, scientists from many fields have focused much attention on the design and preparation of intelligent polymer materials due to their various applications such as drug or gene delivery,[1-3] cancer diagnosis[4] and other biomedical applications.[5] Of the various types of intelligent polymer materials, biologically responsive polymeric prodrugs (BRPPs) have been particularly attractive because of their special properties such as their good stability in blood, higher drug loading, good water solubility and lower cytotoxicity against tumor tissue and cells.[6] Efficacious BRPPs were expected to increase the drug concentration at their sites of action while reducing the drug side effects in non-target tissues, and thus they became a major strategy for improving medical efficiency. In recent years, numerous BRPPs with anticancer drugs that have been covalently conjugated to their micellar cores via cleavable hydrazone, [6-11] esters, [12-17] disulfide[4, 18-20] and other biologically responsive bonds, [21-23] which perfectly combined the stability of prodrugs with the long circulation time of micelles, have been utilized in the development of cancer therapies.

Current polymeric prodrugs are usually amphiphilic polymers that mainly used polyethylene glycol or its derivatives as the hydrophilic component and then a hydrophobic drug was anchored using a biologically responsive bond. Recently, Huynh and co-workers described a new sodium chloride-responsive block copolymer for the release of cisplatin, a cancer drug.[14] Meanwhile, Wang's groups reported one kind of supramolecular polymeric micelle constructed from poly(ethylene glycol)-polypeptide copolymers, which responded to *β*-cyclodextrin[21]. Moreover, Shen and co-workers described esterase-sensitive camptothecin (CPT) prodrug (OEG-DiCPT) micelles with CPT covalently conjugated to a polymeric micelle core via an ester bond, and the drugs showed high in vitro and in vivo antitumor activity.[13] Generally, drugs embedded in or conjugated with inert nanocarriers are expected to show therapeutic advantages over free drugs, but for most polymeric prodrugs, the carrier materials were the major component (generally more than 90%), causing low drug loading contents and thus excessive uses of parenteral excipients[8]. For instance, many reported polymeric prodrugs had very low drug loading capacities (usually less than 10 wt%). [6, 10] So it was a great challenge for researchers to design a more effective system with the attributes of controlled release and higher drug capacity.

To develop more efficacious BRPPs, we herein designed a novel endosomal pH-sensitive doxorubicin (DOX) prodrug based on polyethylene glycol monomethylether-*b*-poly(methacryl amide tert-butyl carbazate-DOX) (MPEG-*b*-DOX) (Scheme 1). Furthermore, polyethylene glycol has been a widely used polymer carrier for drug delivery since it has been approved for clinical use .[24-26] DOX has been grafted to a macromolecular carrier via an acid-labile hydrazone bond, which is known to be sufficiently stable at pH 7.4 but readily cleavable in an acidic environment such as in endo-lysosomes.[27-30] Notably, the MPEG-*b*-DOX copolymers could self-assemble into micelles in aqueous solutions, not only allowing the avoidance of toxic organic solvents but also largely simplify production. The stimuli-responsive release of DOX from MPEG-*b*-DOX prodrugs could take place rapidly, likely due to the fact that polymeric micelles have excellent permeability.[10, 31-32] To study the self-assembly behavior of MPEG-*b*-DOX copolymers, the morphology of MPEG-*b*-DOX micelles was characterized by transmission electron microscopy (TEM). We also investigated the *in vitro* cytotoxicity and cell internalization behavior of the self-assembly micelles. The results indicated that the MPEG-*b*-DOX prodrug had great potential to become a promising DOX drug carrier for cancer treatment.

Results and discussion

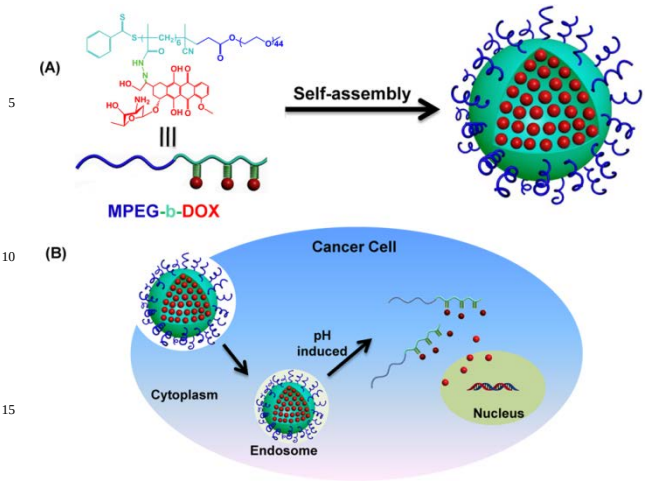

Scheme 1. Schematic illustration of (A) the formation of MPEG-b-DOX micelles and (B) the pH-induced drug release mechanism

The synthesis of MPEG-*b*-DOX copolymers is shown in Fig.S1†. Firstly, the macro RAFT agent, MPEG-CPADB (CPADB: 4-Cyano-4-((thiobenzoyl) sulfanyl)pentanoic acid) was prepared by an esterification reaction, and the ^{1}H NMR and FT-IR results indicated that the MPEG-CPADB was prepared successfully (as shown in Supporting Information). Furthermore, to achieve controlled conjugation of DOX, a new hydrazine bond monomer, methacrylamide tert-butyl carbazate (MABH), was designed and prepared (Fig.S1†). The successful synthesis of MABH was confirmed by ^{1}H NMR spectroscopy, as shown in Fig.S2†, with signals at δ 6.07, 5.42 and 1.96 attributable to the methacrylamide moieties, and resonances at δ 8.22, 6.96 and 1.45-1.93 attributable to tert-butyl carbazate. Then the PEG-*b*-PMABH copolymers were prepared by RAFT polymerization of MABH using MPEG-CPADB as a macro RAFT agent and azobisisobutyronitrile as the radical agent in THF at 60 °C for 24 h. The ^{1}H NMR spectrum of resulting PEG-*b*-PMABH copolymers is shown in Fig.S2†, with the signals at δ 3.38, 3.65 and 4.22 attributable to PEG protons and the signals at δ 7.43, 7.26 and 1.40-1.49 attributable to the MABH proton. According to the ^{1}H NMR spectrum results, the degree of polymerization of MABH was calculated to be 6. In this paper, the block copolymer was referred to as PEG_{43}-$PMABH_6$. Furthermore, the GPC results indicated that the resulting copolymer had a molecular weight close to the value determined from ^{1}H NMR analyses and a low polydispersity of 1.23 (Fig. S3†), indicating successful synthesis of the PEG_{43}-$PMABH_6$ copolymer.

Finally, the MPEG-*b*-DOX prodrug was obtained by treating the deprotected product of PEG-*b*-PMABH (PEG-*b*-hydrazide) with DOX in anhydrous methanol with trace trifluoroacetic acid. The percentage of MABH units conjugated with DOX was about 73.3%, which was determined from the amount of DOX drug loading. The resulting product was confirmed by ^{1}H NMR, FT-IR spectroscopy and high-performance liquid chromatography (HPLC). The signals at δ 7.95-7.96, 7.76-7.80, and 7.66-7.69 were attributable to DOX aromatic group protons (Fig. S2†). Furthermore, the FT-IR spectrum of MPEG-*b*-DOX was expected to offer further evidence of DOX grafting, as shown in Fig. S4†. The peak at 1730 cm^{-1} was due to the carbonyl stretching frequency of free DOX, but the peak was absent in MPEG-*b*-DOX , which indicated the formation of a hydrazone bond between the ketone and hydrazine. [9]

Meanwhile, HPLC was also used to investigate the MPEG-b-DOX. As shown in Fig. S5†, the free DOX had a retention time of 6.73 min, but the MPEG-*b*-DOX did not have a retention time peak, but instead an analytic time of 30 min was used, and this may due to the high molecular weight of MPEG-*b*-DOX. Thus, the result also directly indicated that there was some amount of free DOX in the resulting MPEG-*b*-DOX prodrug, indicating the successful synthesis of the MPEG-*b*-DOX prodrug.

The UV−visible spectrum was used to further understand the conjugation of DOX, as shown in Fig. S6†. The methanol solutions of PEG-*b*-hydrazide had no characteristic peak exept for DOX, which had a characteristic peak at about 500 nm. Compared with DOX, there was no obvious difference in the spectrum of MPEG-*b*-DOX except for a slight red shift. The PEG-*b*-hydrazide in the methanol was colorless, but the color became red after the conjugation of DOX. This phenomenon further demonstrates that only very small amounts of free DOX existed in MPEG-*b*-DOX.

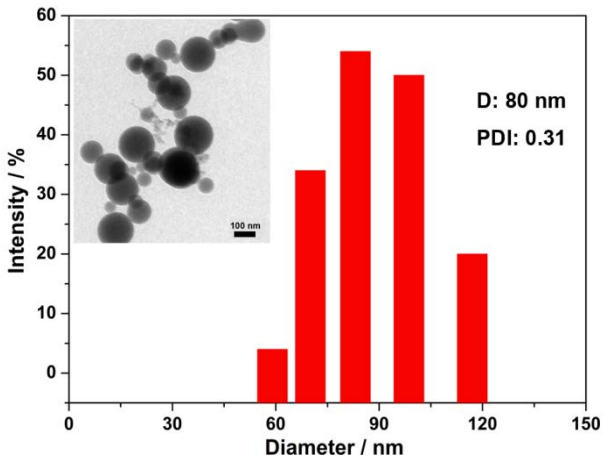

Fig.1. TEM image and size distribution of MPEG-b-DOX micelles.

The loading amount of DOX was further determined using UV-visible absorption spectra following treatment with 1.0 M HCl at room temperature for 24 h. The results indicated that the MPEG-*b*-DOX prodrug had a fixed drug loading content that reached as high as ~ 40 wt%, which is much higher than recent reports regarding DOX prodrugs.[6-7] As shown in Scheme 1, the obtained MPEG-*b*-DOX copolymers could self-assemble to form stable micelles in PBS (pH 7.4) because of their amphiphilic structures. The TEM images (Fig.1) indicate that the MPEG-*b*-DOX micelles exhibited a spherical shape and were ~60 nm in diameter. The size distribution of the micelles was further investigated by DLS (Fig. 1) and their size distribution in water ranged from 52 to 117 nm with an average size of ~80 nm. Furthermore, the micelles had a ζ-potential of +2.1 mV. Such nanosized MPEG-*b*-DOX micelles could easily avoid renal filtration, leading to prolonged residence time in the bloodstream which allows more effective targeting of diseased tissues.[33-36]

Compared with the reported water-soluble polymer-DOX

prodrugs or conjugates, the resulting MPEG-*b*-DOX prodrug was so different from these. For example, a low molecular weight hydrophilic PEG polymer was used to reduce the proportion of inert nanocarriers and ensured both a high drug loading content and the water-solubility of prodrugs. Moreover, the PEG polymer could effectively reduce non-specific uptake by the reticuloendothelial system (RES), prolong circulation time and allow for specific tumor-targeting through the enhanced permeability and retention (EPR) effects .[8, 37]

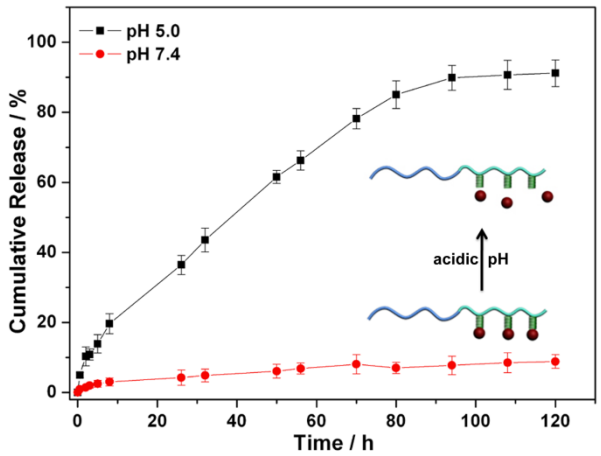

Fig. **2**. In vitro release of DOX from MPEG-*b*-DOX micelles in different pH PBS solution at 37 °C

The *in vitro* release of DOX from the MPEG-*b*-DOX prodrug was evaluated at 37 °C in different buffers (pH 5.0 and 7.4) and the results are shown in Fig. 2. The results indicate that drug release under mildly acidic environments was significantly faster than that at neutral pH because of the hydrazone bond. For example, approximately 91.2% of DOX was released in 120 h at pH 5.0 from MPEG-*b*-DOX; however, only 8.8% of DOX was released at pH 7.4 under the same conditions. These results indicated that the MPEG-*b*-DOX prodrug was very stable under physiological conditions and was quickly responded to the endo/lysosomal environment. The slow drug release from the MPEG-*b*-DOX prodrug micelles may indicate that the hydrophobic micellar core is a physical barrier for the diffusion of acid into the micelles as well as for the diffusion of cleaved DOX out of the micelles.[10]

The biocompatibility of the PEG-*b*-hydrazide carrier was investigated in the human tongue squamous cell carcinoma (TCA8113) cell line and rat adrenal pheochromocytoma (PC12) cell line by an SRB assay. The cytotoxicity results demonstrated that the PEG-*b*-hydrazide carrier was basically nontoxic to both TCA8113 and PC12 cancer cells at a tested concentration of up to 800 μg/mL (Fig. 3A), indicating its excellent biocompatibility, which demonstrated that the PEG-*b*-hydrazide carrier was suitable for potential application *in vivo*.

In contrast to these results, the MPEG-*b*-DOX prodrug exhibited higher cytotoxic effects (Fig.3B), which revealed that the MPEG-*b*-DOX prodrug exhibited significant *in vitro* antitumor activity. For examples, the half maximal inhibitory concentration (IC_{50}) values for MPEG-b-DOX against the TCA8113 and PC12 cancer cells were 8.9 and 4.2 μg/mL, respectively. While those for free DOX were 0.6 and 6.4 μg/mL respectively. Notably, free DOX was passed through cellular and nuclear membranes by passive diffusion. But the MPEG-*b*-DOX prodrug, which was expected to enter into cancer cells by endocytosis, actually followed a very slow endo/lysosomal process that was followed by drug distribution in cells.[38] Because of the slow release of DOX from the MPEG-*b*-DOX prodrug, the transport process of the MPEG-*b*-DOX prodrug was slower than passive diffusion. Considering the controlled release results, the phenomenon was reasonable. The results also indicated that the MPEG-*b*-DOX prodrug successfully served as a platform to carry DOX into cells, resulting in an expected anticancer effect.

To elucidate the cell uptake of MPEG-*b*-DOX prodrug micelles for intracellular drug delivery, the internalized distribution of free DOX and the MPEG-b-DOX prodrug micelles in TCA8113 cancer cells was monitored by laser scanning confocal microscopy (LSCM). The fluorescence (shown in red) of DOX was observed at different incubation time. Meanwhile, DAPI was used to label the cell nucleus (shown in blue). As revealed by LSCM studies (Fig. 4A-C), no red fluorescence was observed in the TCA8113 cancer cells following a 3 h incubation with the MPEG-*b*-DOX prodrug (Fig. 4A).

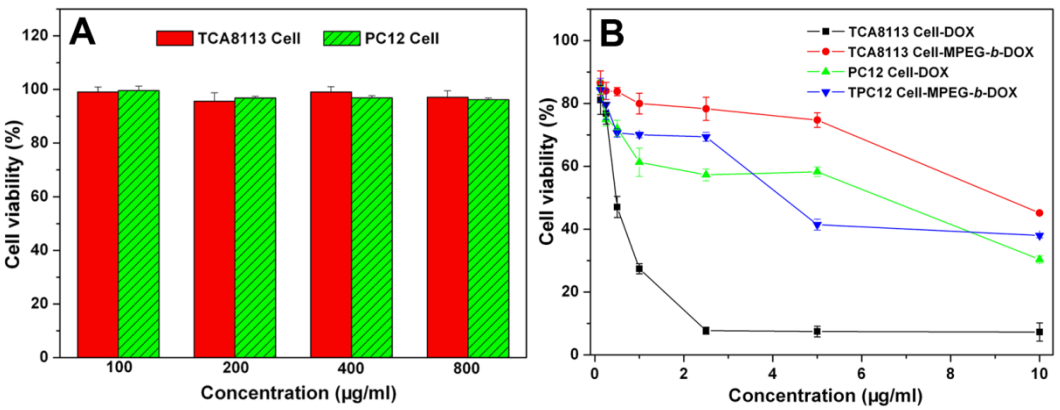

Fig.3. (A) Cytotoxicity of MPEG-b-hydrazide at varying concentrations of 100, 200, 400 and 800 μg/mL. TCA8113 and PC12 tumor cell were incubated with MPEG-b-hydrazide for 24 h. (B) Cytotoxicity of MPEG-b-DOX and free DOX at varying concentrations of 0.125—10 μg equiv/mL. TCA8113 and PC12 tumor cells were incubated with MPEG-b-DOX and free DOX for 24 h. The cell viability was determined by SRB assay. Data represent mean ±

standard deviations (SD) (n = 3).

However, after a longer incubation time, such as 24 h, the fluorescence of DOX became almost invisible in the cytoplasm and nucleus of the TCA8113 cancer cells (Fig. 4B), and this indicated an endo/lysosomal process was the pathway of entry for MPEG-*b*-DOX micelles into the cells. As shown in Fig.S7 (see the high magnification images), many MPEG-*b*-DOX micelles were found entering into cells gradually, revealing the controlling release process of DOX. In contrast, free DOX was distributed to the perinuclei and nuclei of the TCA8113 cancer cells after 3 h (Fig. 4C), which also revealed a passive diffusion entry process for free DOX. However, after a longer incubation time of 24 h, we found more free DOX entered into cancer cells, and accumulated in nuclei (Fig. 4D), corresponding to the results of cytotoxicity. For MPEG-*b*-DOX prodrug micelles, cellular uptake was mainly based on the small size and the endocytosis mechanism which may result in a greater number of prodrug micelles entering into cells gradually, and showing a continued cytotoxic effect. A considerably a longer time was needed for the MPEG-*b*-DOX prodrug to carry DOX into the cells compared to the direct application of free DOX. The MPEG-*b*-DOX prodrug may provide a promising platform for prolonged circulation as well as tumor-targeted drug delivery by utilizing the EPR effect and introducing targeting ligands into prodrugs.

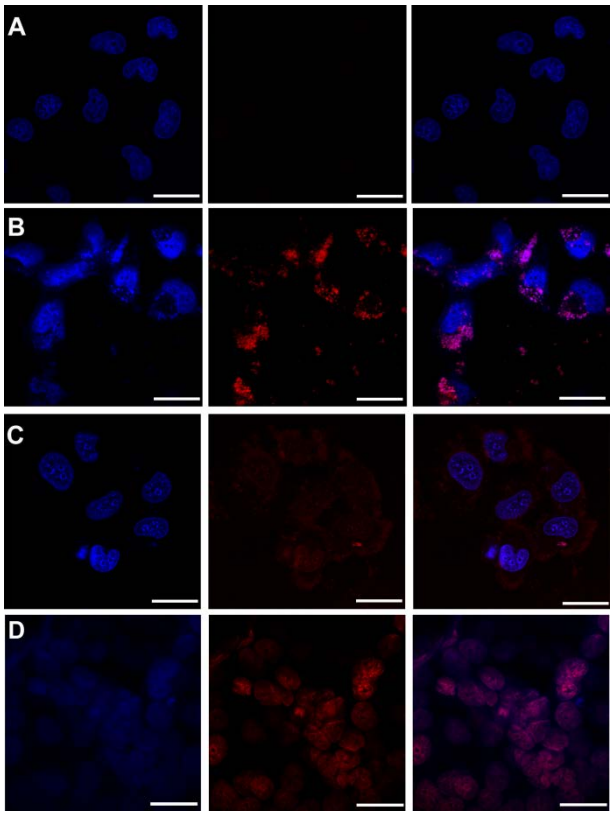

Fig.4. LSCM images of TCA8113 cancer cells incubated with MPEG-b-DOX prodrug and free DOX (5 μg equiv/mL). For each panel, the images from left to right show DOX fluorescence in cell nuclei stained by DAPI (blue), cells (red) and overlays of the two images. (A) MPEG-b-DOX prodrug, 3 h incubation (B) MPEG-b-DOX prodrug, 24 h incubation (high magnification imagesare shown in Figure S7 in Supporting Information)., (C) free DOX, 3 h incubation and (D) free DOX, 24 h incubation. The scale bars correspond to 30 μm in all images.

Conclusions

In summary, we have described a strategy for preparing a novel MPEG-b-DOX prodrug that reduces the proportion of inactive materials and to minimize drug leakage. The MPEG-*b*-DOX prodrug formed micelles in aqueous solutions and had a high drug loading (~ 40 wt%). Furthermore, the resulting micelles were very stable with minimal drug release at pH 7.4 but high release DOX at pH 5.0. Further studies indicated that the MPEG-*b*-DOX had high anticancer activity against the TCA8113 cells and PC12 cells. The cell imaging studies showed that the MPEG-*b*-DOX prodrug could be tracked at the cellular level for anticancer therapy. This integration of functional components may result in the MPEG-*b*-DOX prodrug becoming a promising multifunctional carrier for controlled drug delivery applications.

Acknowledgements

This work was financially supported by National Science Foundation (No.21375052) and the National Science Foundation for Fostering Talents in Basic Research of the National Natural Science Foundation of China (Grant No. J1103307)

Notes and references

*[a]State Key Laboratory of Applied Organic Chemistry, Lanzhou University, Lanzhou 730000, China; [b]School of Chemical and Biomedical Engineering, Nanyang Technological University, 70 Nanyang Drive, Singapore 637457; [c] School of Basic Medical Science, Lanzhou University, Lanzhou 730000, China.
Tel.: +86 931 8912510; fax: +86 931 8912582. E-mail address: zhanghx@lzu.edu.cn (Haixia Zhang) .

† Electronic Supplementary Information (ESI) available: [The experimental details on the synthesis and characterization of the resulting DOX prodrug; the GPC result of PEG_{43}-b-$PMABH_6$ copolymer; the FTIR, UV-vis spectra and HPLC curves of DOX and PEG-b-DOX.]. See DOI: 10.1039/b000000x/

1 E. Segal and R. Satchi−Fainaro, *Adv. Drug Deliv. Rev.*, 2009, *61*, 1159−1176.
2 G. Pasut, F. M. Veronese, *Adv. Drug Deliv. Rev.*, 2009, *61*, 1177−1188.
3 A. E. Felber, M. H. Dufresne and J. C. Leroux, *Adv. Drug Deliv. Rev.*, 2012, *64*, 979−992.
4 M. H. Lee, J. Y. Kim, J. H. Han, S. Bhuniya, J. L. Sessler, C. Kang and J. S. Kim, *J. Am. Chem. Soc.*, 2012, *134*, 12668−12674.
5 M. H. Lee, J. H. Han, P. S. Kwon, S. Bhuniya, J. Y. Kim, J. L. Sessler and J. S. Kim, *J. Am. Chem. Soc.*, 2012, 134, 1316−1322.
6 L. Zhou, R. Cheng, H. Tao, S. Ma, W. Guo, F. Meng and Z. Zhong, *Biomacromolecules*, 2011, *12*, 1460−1467.
7 J. Z. Du, X. J. Du, C. Q. Mao and J. Wang, *J. Am. Chem. Soc.*, 2011, *133*, 17560− 17563.
8 P. F. Gou, W. W. Liu, W. W. Mao, J. B. Tang, Y.Q. Shen and M. H. Sui, *J. Mater. Chem. B*, 2013, *1*, 284−292.
9 N.V. Rao, S. Mane, A. Kishore, J. Das Sarma and R. Shunmugam, *Biomacromolecules*, 2012, *13*, 221−230.
10 F. Zhan, W. Chen, Z. Wang, W. Lu, R. Cheng, C. Deng and Z. Zhong, *Biomacromolecules*, 2011, *12*, 3612−3620.
11 K. Sakai−Kato, K. Ishikura, Y. Oshima, M. Tada, T. Suzuki, A. Ishii−Watabe and H. Okuda, *Int. J. Pharmaceut.*, 2012, *423*, 401−409.

12 J. A. Johnson, Y. Y. Lu, A. O. Burts, Y. Xia, A. C. Durrell, D. A. Tirrell and R. H. Grubbs, *Macromolecules*, 2010, *43*, 10326−10335.

13 Shen, E. Jin, B. Zhang, C. J. Murphy, M. Sui, J. Zhao and W. J. Murdoch, *J. Am. Chem. Soc.*, 2010, *132*, 4259−4265.

14 V. T. Huynh, J. Y.Quek, P. L. de Souza and M. H. Stenzel, *Biomacromolecules*, 2012, *13*, 1010−1023.

15 L. Mao, H. Wang, M. Tan, L. Ou and D. Kong, *Chem. Commun.*, 2011, *48*, 395−397.

16 M. E. Fox, S. Guillaudeu, J. M. Fréchet, K. Jerger, N. Macaraeg and F. C. Szoka, *Mol. Pharmaceut.*, 2009, *6*, 1562−1572

17 S. K. Pawar, A. J. Badhwar, F. Kharas, J. J. Khandare and P. R. Vavia, *Int. J. Pharmaceut.*, 2012, *436*, 183−193.

18 A. G. Cheetham, P. Zhang, Y. A. Lin, L. L. Lock and H. Cui, *J. Am. Chem. Soc.*, 2013, *135*, 2907−2910.

19 H. Wei, J. G. Schellinger, D. S. Chu and S. H. Pun, *J. Am. Chem. Soc.*, 2012, *134*, 16554−16557.

20 A. W. Jackson and D. A. Fulton, *Macromolecules*, 2012, *45*, 2699−2708.

21 F. Greco, I. Arif, R. Botting, C. Fante, L. Quintieri, C. Clementi, O. Schiavon, G. Pasut, *Polym. Chem.*, 2013, 4, 1600−1609.

22 M. Naito, T. Ishii, A. Matsumoto, K. Miyata, Y. Miyahara and K. Kataoka, *Angew. Chem. Int. Ed.*, 2012, *51*, 10751 –10755.

23 M. Bio, G. Nkepang and Y. You, *Chem. Commun.*, 2012, *48*, 6517−6519.

24 F. M. Veronese, O. Schiavon, G.Pasut, R. Mendichi, L. Andersson, A. Tsirk, J. Ford, G. F. Wu, S. Kneller, J. Davies and R. Duncan, *Bioconjugate Chem.*, 2005, *16*, 775–784.

25 R. B. Greenwald, Y. H. Choe, J. McGuire and C. D. Conover, *Adv. Drug Deliv. Rev.*, 2003, *55*, 217–250.

26 C. Y. Long, M. M. Sheng, B. He, Y. Wu, G. Wang and Z. W. Gu, Chin. *J. Polym. Sci.*, 2012, *30*, 387–396

27 M. Hruby, C. Konak and K.Ulbrich, *J. Control. Release.*, 2005, *103*, 137–148.

28 Y. Bae, S. Fukushima, A. Harada and K. Kataoka, *Angew. Chem. Int. Ed.*, 2003, *42*, 4640− 4643.

29 X. L. Hu, S. Liu, Y. B. Huang, X. S. Chen and X. B. Jing, *Biomacromolecules*, 2010, *11*, 2094−2102.

30 C. C. Lee, E. R.Gillies, M. E. Fox, S. J. Guillaudeu, J. M. J.Frechet, E. E. Dy and F. C. Szoka, *Proc. Natl. Acad. Sci. U. S. A.*, 2006, *103*, 16649−16654.

31 K. Raemdonck, J. Demeester and S. De Smedt, *Soft Matter.*, 2009, *5*, 707−715.

32 J. K. Oh, R. Drumright, D. J. Siegwart and K. Matyjaszewski, *Prog. Polym. Sci.*, 2008, *33*, 448−477.

33 Z. G. Xu, D. D. Wang, M. Guan, X. Liu, Y. J. Yang, D. F. Wei and H. X. Zhang, *ACS Appl. Mater. Interfaces*, 2012, *4*, 3424−3431.

34 J. H. Park, L. Gu, G. vonMaltzahn, E. Ruoslahti, S. N. Bhatia and M. Sailor, *J. Nat. Mater.*, 2009, *8*, 331−336.

35 W. T. Wu, J. Shen, P. Banerjee and S. Q. Zhou, *Biomaterials*, 2010, *31*, 8371− 8381.

36 K. E. Schmalenberg, L. Frauchiger, L. Nikkhouy−Albers and K. E. Uhrich, *Biomacromolecules*, 2001, *2*, 851−855.

37 G. Molineux, *Cancer Treat. Rev.* 2002, *28*, 13–16.

38 N. Tang, G. J. Du, N. Wang, C. C. Liu, H. Y. Hang and W. Liang, *J. Natl. Cancer Inst.*, 2007, *99*, 1347−1361.

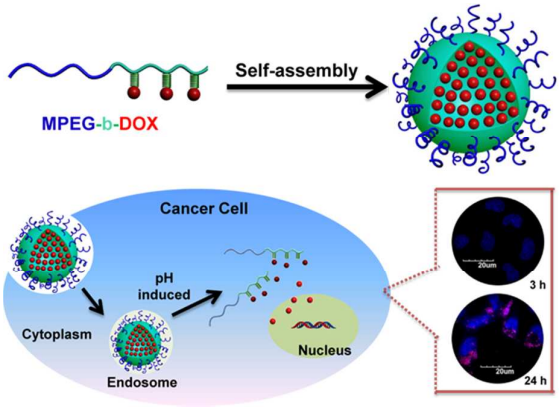

A novel doxorubicin (DOX) prodrug (MPEG-b-DOX) was synthesized with expect to reducing the proportion of inactive materials and minimizing drug leak.